# Study of crystallization process of soda lead silicate glasses by thermal and spectroscopic methods

Oana Cătălina Mocioiu · Maria Zaharescu ·
Irina Atkinson · Ana-Maria Mocioiu ·
Petru Budrugeac

**Abstract** The crystallization process of some glasses in the ternary $Na_2O$–$SiO_2$–$PbO$ system with good chemical stability that can be used for waste inertization was studied using X-ray diffraction (XRD), infrared spectroscopy (FT-IR), differential thermal analysis (DTA) and scanning electron microscopy. The parent glasses were characterized by XRD and FT-IR, and their vitreous state was determined. DTA measurements evidenced glass transition ($T_g$) and crystallization temperatures ($T_c$). The thermal treatments were conducted at vitreous transition temperature (400 °C) and at highest effect of crystallization (650 °C). XRD evidenced the lead and sodium silicate crystalline phases in samples treated at 650 °C for 12 h. Micrometer crystallites dispersed in the glass matrices have affected the transparence of glasses and made them opaque after treatment at 650 °C. The influence of oxide quantities in compositions on the crystallization tendency was revealed. A PbO higher content than that of $SiO_2$ as well as lower $Na_2O$ content decreased the tendency of crystallization.

O. C. Mocioiu (✉) · M. Zaharescu · I. Atkinson
"Ilie Murgulescu" Institute of Physical Chemistry of the
Romanian Academy, 202 Splaiul Independentei Street,
060021 Bucharest, Romania
e-mail: oana.mocioiu@yahoo.com

A.-M. Mocioiu
Department of Research and Materials Investigation, National
R&D Institute of Textile and Leather, 16 Lucretiu Patrascanu
Street, Bucharest, Romania

P. Budrugeac
Advanced Research Institute for Electrical Engineering,
INCDIE-ICPE-CA, 313 Splaiul Unirii Street, Bucharest,
Romania

## Introduction

Many authors have intensively studied the crystallization process of glasses to apply the results in industrial processes [1–12]. The properties of glass–ceramics are determined by the crystallization phases precipitated from the glasses and their microstructures, which depended on composition of the parent glasses as well as thermal treatment [13–16].

It is well known that the nucleation mechanisms in glasses are different and they are influenced by chemical composition. Most glasses crystallize heterogeneously from the external surface to the internal part and only few crystallize homogeneously in bulk [17]. The crystallization of glasses can be homogeneous when this phenomenon begins from critical nuclei formation on surface or in volume or heterogeneous when nucleation of foreign solid particles or phase boundaries occurs [18, 19].

Glasses that are obtained by cooling homogeneous (single phase) liquids are generally transparent, but many of them have a heterogeneous structure on a submicroscopic scale [16]. This "microphase separation" is found in numerous binary and ternary silicate and borate systems (e.g. $Na_2O$–$SiO_2$, $Li_2O$–$SiO_2$, $Na_2O$–$CaO$–$SiO_2$, etc.) [3, 6, 8]. The authors found that phase separation increases the crystal nucleation and growth rates.

Concerning structure, Zanotto [20] have included the $SiO_2$–$Na_2O$ glass system in glasses that nucleate homogeneously and $SiO_2$–$PbO$ glass system in glasses that nucleate heterogeneously. Due to this fact, in the ternary system, the crystallization could be complex and surely depend on

**Table 1** Chemical composition of samples and XRF results obtained on parent glasses

| Glass | Chemical composition/mass% | | | XRF results/% at | | | | | Na$_2$O calculated from XRF/mass% |
|---|---|---|---|---|---|---|---|---|---|
| | SiO$_2$ | PbO | Na$_2$O | Si | Pb | Na | O | C | |
| A$_3$ | 35 | 44 | 21 | 11.51 | 35.34 | 11.44 | 35.15 | 6.56 | 20.23 |
| B$_3$ | 44 | 35 | 21 | 14.36 | 33.98 | 9.75 | 36.83 | 5.07 | 18.96 |
| A$_2$ | 35 | 40 | 25 | 11.08 | 36.02 | 11.39 | 36.38 | 5.13 | 20.48 |
| B$_2$ | 40 | 35 | 25 | 13.67 | 30.00 | 12.70 | 37.90 | 5.72 | 22.18 |
| D$_1$ | 45 | 30 | 25 | 17.95 | 28.62 | 11.27 | 37.95 | 4.21 | 20.76 |
| D$_3$ | 50 | 25 | 25 | 17.83 | 30.39 | 10.87 | 37.07 | 3.84 | 20.41 |

the ratio of Na and Pb in the composition. Some attempts to bring information on the matter were realized previously by the authors [21]. Due to the complex crystallization process of the most studied compositions, kinetic calculations were possible for only one glass [21].

In this paper, we report the study of the crystallization process of some glasses in the ternary Na$_2$O–SiO$_2$–PbO system with good chemical stability that can be used for waste inertization as presented by authors in a previous paper [22].

## Experimental procedure

### Parent glass preparation

Glass batches of 100 g having mass–percentage compositions of PbO, SiO$_2$ and Na$_2$CO$_3$ were prepared. The materials were reagent-grade chemicals from MERCK. Glass batches were well mixed in a mill and then melted in Pt crucible for 1 h at 1,400 °C in an electrically heated furnace. The melts were poured into a preheated mould to obtain glass.

The chemical compositions of parent glasses in this paper were chosen to reproduce the samples with good chemical stability for waste inertization [22], and they are displayed in Table 1.

The volatilisation of elements during the melting of the parent glasses was determined by wavelength dispersive X-ray fluorescence (WDXRF) spectroscopy method (XRF). The Rigaku ZSX Primus II spectrometer is equipped with an X-ray tube with Rh anode, 4.0 kW power, with front Be window, and a thickness of 30 μm. A set of seven analysing crystals (LiF200, LiF220, PET, Ge and 3 multi-layer crystals) facilitates qualitative and quantitative analyses of elements ranging from beryllium (Be) through uranium (U). The XRF data were analysed using EZ scan combined with Rigaku's SQX fundamental parameters software (standard less), which is capable of
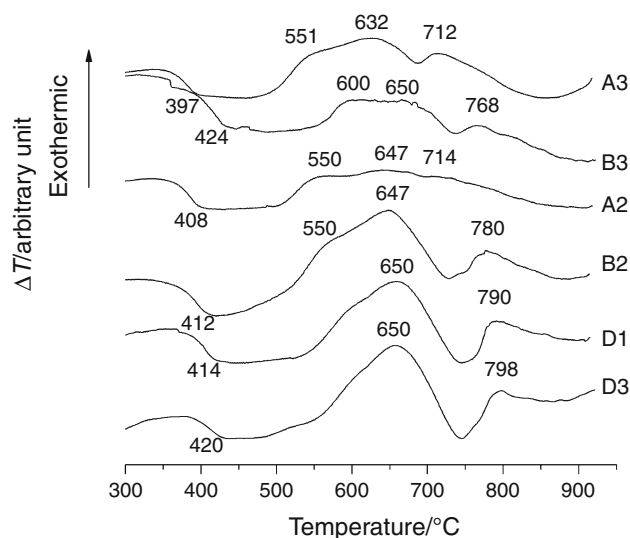


**Fig. 1** Differential thermal analysis of studied glasses recorded in static air

automatically correcting for all matrix effects, including line overlaps. The samples for XRF measurements were prepared starting from fine powders by pressing them in a ring with a diameter of 1 cm. The elemental analyses results and mass loss of sodium oxide are given in Table 1. The volatility of sodium oxide was between 0.6 and 5 mass%. The volatility can be less than the calculated values due to the percentage of C impurity of 4.20–6.56 mass% adsorbed from the atmosphere. In all samples recorded on the apparatus, C impurity was observed. Even for loss of 5 mass%, the results were not compromised because the compositions have been in the same subsystem according with phase diagram of ternary system [23].

### Glass crystallization

All samples were treated for 12 h at vitreous transition temperature (400 °C) and at crystallization temperature

**Table 2** Temperatures in DTA curves of parent glasses, their assignment and crystalline phases obtained after thermal treatment at 650 °C for 12 h

| Glass | Glass transition temperature $T_g$/°C | Crystallization temperature $T_c$/°C | Crystalline phase after treatment at 650 °C for 12 h |
|---|---|---|---|
| A3 | 397 | 551 | $Pb_3Si_2O_7$ |
|  |  | 632 | $Na_2Si_2O_5$ (monoclinic) |
|  |  | 712 |  |
| B3 | 424 | 600 | $Pb_3Si_2O_7$ |
|  |  | 650 | $Na_2Si_2O_5$ (monoclinic) |
|  |  | 768 | $Na_2Si_2O_5$ (orthorhombic) |
| A2 | 408 | 550 | $Pb_3Si_2O_7$ |
|  |  | 647 | $Na_2Si_2O_5$ (monoclinic) |
|  |  | 714 |  |
| B2 | 412 | Shoulder 550 | $Pb_3Si_2O_7$ |
|  |  | 647 | $Na_2Si_2O_5$ (monoclinic) |
|  |  | 780 | $Na_2Si_2O_5$ (orthorhombic) |
| D1 | 414 | Shoulder 570 | $Pb_3Si_2O_7$ |
|  |  | 650 | $Na_2Si_2O_5$ (monoclinic) |
|  |  | 790 | $Na_2Si_2O_5$ (orthorhombic) |
| D3 | 420 | Shoulder 570 | $Pb_3Si_2O_7$ |
|  |  | 650 | $Na_2Si_2O_5$ (monoclinic) |
|  |  | 798 | $Na_2Si_2O_5$ (orthorhombic) |

(650 °C). Heating rate was 10 °C min$^{-1}$ and the natural cooling to room temperature followed the treatment. The crystallization program was established based on the differential thermal analysis presented below.

Characterisation techniques

### Differential thermal analysis

The thermal properties were studied by a differential thermal analysis, using Q-1500D apparatus with α-alumina powder as a reference material. The ground powders of six different glasses of diameter between 0.3 and 0.5 mm were heated in a platinum pan at a heating rate of 10° min$^{-1}$, in the range 25–1,000 °C, in static air atmosphere. The glass transition temperatures were determined from the tangent intersections of baseline change due to caloric capacity changing in the DTA curves. The crystallization temperatures were obtained from the temperatures of the exothermic peak.

### X-ray diffraction (XRD)

The XRD of the parent glasses and the crystallized ones was examined on powdered samples using a Rigaku Ultima IV diffractometer, in parallel-beam geometry. The X-ray experiments were carried out with a Cu tube
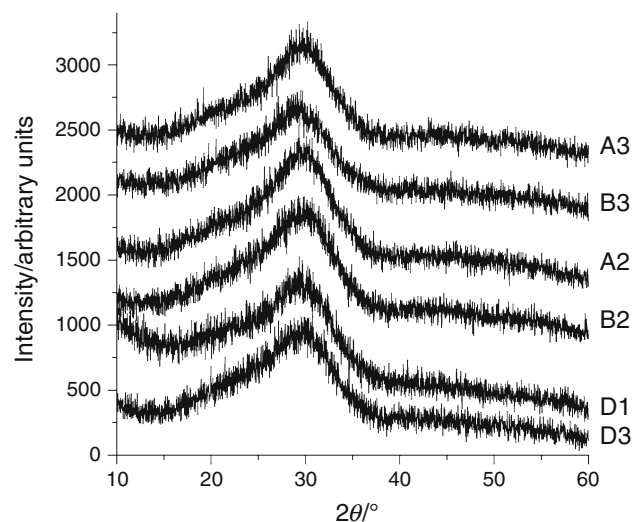


**Fig. 2** XRD patterns of samples treated at 400 °C for 12 h

($\lambda = 1.5406$ Å) operating at 40 kV and 30 mA. Counts were collected from 10° to 60° with a step size of 0.02 and a speed of 5° min$^{-1}$. The glassy state was evidenced for initial samples from the shape of record. Crystallites were identified from peak's position in cases of samples treated at crystallization temperature. Phase identification was performed using Rigaku's PDXL software connected to ICDD PDF-2 database.

*Infrared spectroscopy (FT-IR)*

FT-IR spectra for powder of parent glasses and of treated samples were recorded between 400 and 1,600 $cm^{-1}$, on the KBr transparent pellet with a NICOLET 6700 apparatus, using 16 scans. The error in position of a band was at 4 $cm^{-1}$.

*Scanning electron microscopy (SEM) and energy-dispersive X-ray (EDAX)*

Scanning electron microscopy (SEM) using a high-resolution microscope Quanta Fei 200 model coupled with energy dispersive X-ray (EDAX) analysis investigated the microstructure of the samples.

## Results and discussions

Thermal analysis

The differential thermal analysis curves for glasses are presented in Fig. 1. In all samples, the first baseline change in the DTA curve near 400 °C implies the glass transition temperature ($T_g$); the next broad exothermic effects are attributed to the crystallization ($T_c$) or phase transformation of crystal structure. The DTA curves exhibit two or three crystallization effects: a major crystallization effect at 650 °C and a shoulder at 550 or 600 °C as well as an effect after 710 °C. The characteristic temperatures for all glasses are presented in Table 2.

Glass transition temperature ($T_g$) where the ordering of structure occurs due to decreasing viscosity during the heating was a change of baseline in all DTA curves. Differential thermal analysis of A2 glass and A3 glass showed $T_g$ at 397 and 408 °C. The glass transition of B2, B3, D1 and D3 glasses occurred at 412, 414, 420 and 424 °C. The lower temperatures of glass transition for A2 and A3 glasses can be correlated to a higher content of PbO than that of $SiO_2$ in composition and to the behaviour of PbO as flux.

The exothermic effects in the DTA curves imply that crystalline phases were crystallized during the treatment, and these crystalline phases were confirmed by XRD results. In all DTA curves, the exothermic effects were overlapping.

The literature data reported the crystallization of natrosilite at 630–650 °C [16] and of barysilites at 500 °C [17], in binary glasses. The temperatures are in good agreement with our DTA results of studied glasses (see Fig. 1; Table 2).

In DTA curves of studied glasses, the first exothermic effect in the range 500–600 °C can be correlated with crystallization of barysilite. The second exothermic effect in the range of 630–650 °C and the third effect in the range of 712–800 °C show the crystallization of natrosilite.

The crystalline sodium silicates such as $Na_2Si_2O_5$ have been studied because of their high ion-exchange capacity and selectivity (Wolf and Schwieger 1979) and of their two-dimensional sodium diffusion and conductivity (Heinemann and Frischat 1990) [24]. Depending on synthesis conditions and temperature, different polymorphs of $Na_2Si_2O_5$ (phases α, β, γ, δ) can appear at ambient pressure [25, 26]. The temperature 715 °C was reported as triple point of natrosilite where the three α, β and γ polymorph phases are in thermodynamic equilibrium at 90 barr [27]. According to studies, the γ-phase shows a reversible phase transformation at about 563 °C at ambient pressure [24–26]. According to Shahid and Glasser [28] at 700 °C, the phase transformation from β-$Na_2Si_2O_5$ into α-phase occurs. Single crystal photographs indicated a pseudo-orthorhombic, monoclinic primitive lattice with $a = 4.9$, $b = 23.4$, $c = 15.4$ Å and angle of 90° [24, 28]. The phase α-$Na_2Si_2O_5$ has two reversible transitions at 678 and 707 °C due to minor distortions of the $SiO_4$ groups and rotations of the tetrahedra [24, 25].

In the DTA curves of the ternary system, the A3 sample has effects shifted to lower temperatures as a result of lower $SiO_2$ and $Na_2O$ contents. In samples when the $SiO_2$ content is lower than PbO content (A2 and A3 glasses), the intensities of exothermic effects showing crystallization decrease and the number of crystals decreases, as can be seen in the SEM images presented below (Fig. 5a–f). In ternary glasses with 25 mass% $Na_2O$, the third exothermic effect representing crystallization was shifted to higher temperatures with decreasing PbO content in composition.

The glass transition temperature of 400 °C ($T_g$) and the temperature of higher crystallization effect at 650 °C ($T_c$) were chosen for thermal treatment to investigate crystallization in glasses.

XRD results

All parent glasses exposed vitreous state and even after thermal treatment at 400 °C for 12 h they remained amorphous. In Fig. 2, the XRD patterns of glasses treated at 400 °C for 12 h are presented. The XRD results of parent glasses were identical (they are not presented here). According to Zanotto [20], homogeneous nucleation occurs in glasses when temperature of maximum nucleation rate is higher than glass transition temperature ($T_g$). The XRD pattern of studied glasses treated at 400 °C has shown glassy state and concluded that their maximum nucleation rate is higher than $T_g$.

According to the conclusion of DTA and XRD results, the ternary $SiO_2$–$PbO$–$Na_2O$ glass system seems to exhibit homogenous nucleation compared to $SiO_2$–$PbO$ binary glass system, which presents heterogeneous nucleation, and the binary $SiO_2$–$Na_2O$ glass system, which has homogenous nucleation.

Figure 3a–e shows the XRD results of samples treated at 650 °C (crystallization temperature) for 12 h.

The higher crystallization tendency could be observed in glasses, namely D1 and D3. Their intensities of peak at $2\theta$ of 23.09° are two or three times higher than of other samples treated at 650 °C for 12 h. The lower intensity of peaks in XRD patterns was observed in the A2, A3 and B3 glasses, implying the lower crystallization and the best thermal resistance. The XRD results are in agreement with DTA results that have shown lesser exothermic effects for these three glasses. The XRD results revealed the presence of three crystalline phases. The crystalline phases found in XRD pattern of samples treated at 650 °C are sodium disilicate (natrosilite) in two coordinations, $Na_2Si_2O_5$—monoclinic (reference code 00-023-0529), $Na_2Si_2O_5$—orthorhombic (reference code 01-076-0784), and barysilite ($Pb_3Si_2O_7$; reference code 00-032-0536).



Fig. 3 XRD patterns of samples treated at 650 °C for 12 h: a A3; b B3; c A2; d B2; e D1; f D3 (black circle $Na_2Si_2O_5$—monoclinic; circle $Na_2Si_2O_5$—orthorhombic; asterisk $Pb_3Si_2O_7$)
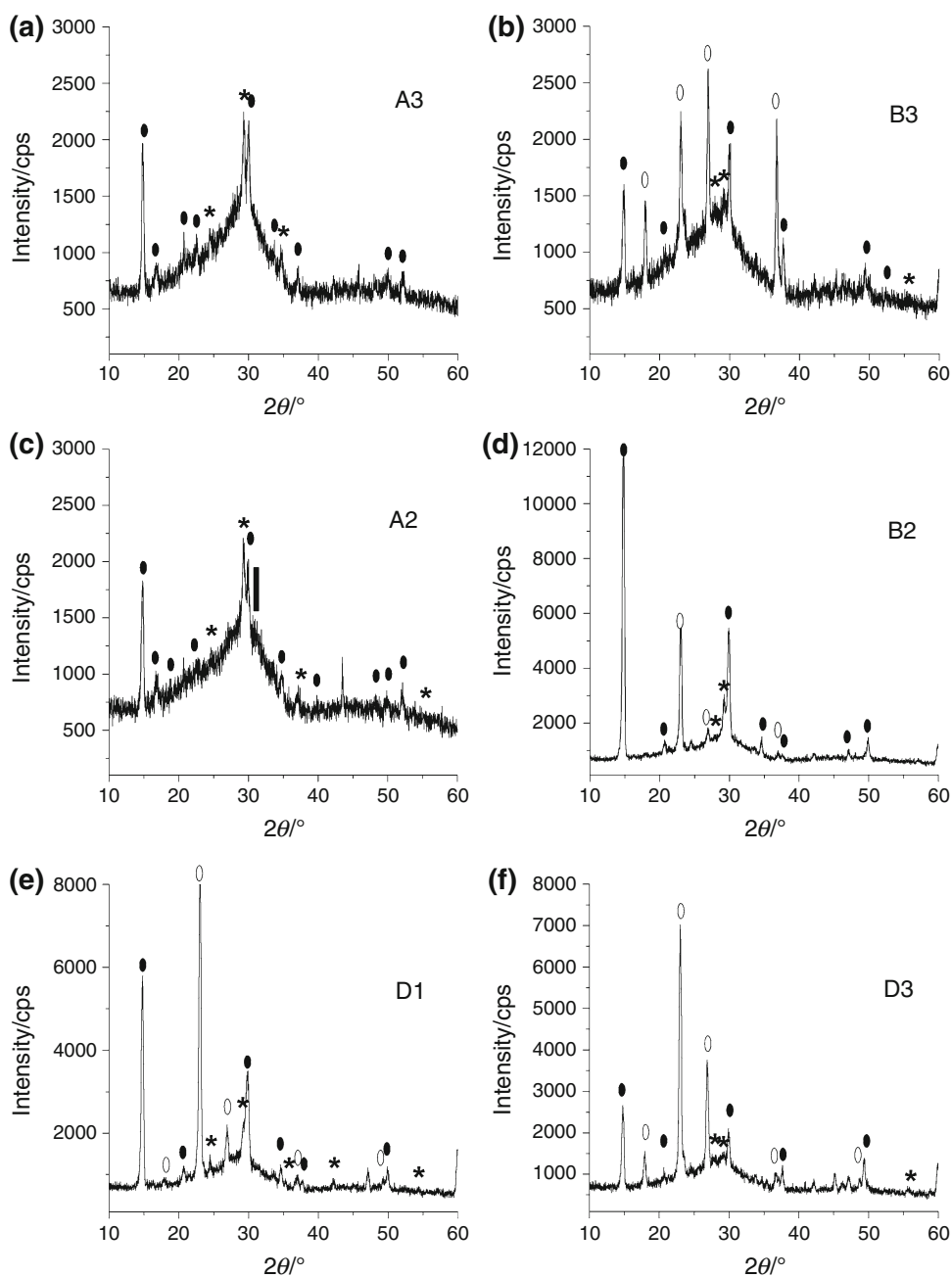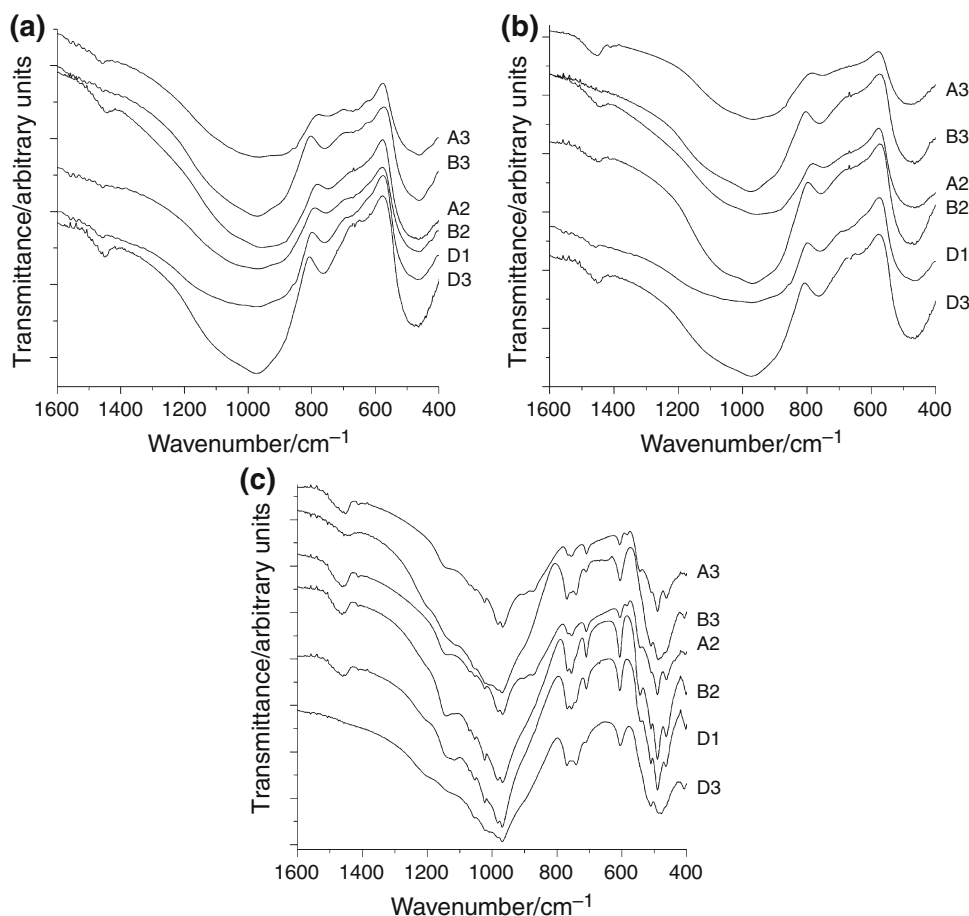
**Fig. 4** FT-IR spectra: **a** parent glasses; **b** the samples treated at 400 °C for 12 h and **c** the samples treated at 650 °C for 12 h

The results obtained are in agreement with thermodynamic data. It is well known that free energy changes are associated with crystal formation and that the most stable nuclei have lower free energy. The literature data give $\Delta_fG = -2{,}324$ kJ mol$^{-1}$ for formation of Na$_2$Si$_2$O$_5$ [29] and $\Delta_fG = -2{,}441$ kJ mol$^{-1}$ for formation of Pb$_3$Si$_2$O$_7$ [30]. The explanation for crystallization of Na$_2$Si$_2$O$_5$ and Pb$_3$Si$_2$O$_7$ can be the formation of stable nuclei due to their low free energy compared with the formation of other silicates in studied glasses. The Gibbs free energy for other silicates is: $\Delta_fG = -1{,}460$ kJ mol$^{-1}$ for formation of Na$_2$SiO$_3$ [29]; $\Delta_fG = -1{,}972$ kJ mol$^{-1}$ for formation of Na$_4$SiO$_4$ [29]; $\Delta_fG = -1{,}093$ kJ mol$^{-1}$ for formation of PbSiO$_3$ [30]; and $\Delta_fG = -1{,}379$ kJ mol$^{-1}$ for formation of Pb$_2$SiO$_4$ [30].

In ternary system, for the A2 and A3 samples with a content of PbO higher than that of SiO$_2$, the peak intensities in XRD patterns are the same for lead silicate and sodium silicate crystals. Also just monoclinic natrosilite was present in samples treated at 650 °C for 12 h. The conclusion can be that high content of lead oxide in composition promotes the crystallization of monoclinic natrosilite in samples treated at 650 °C.

In all samples with SiO$_2$ content higher than that of PbO content after treatment at 650 °C for 12 h near barysilite crystallize a mixture of monoclinic and orthorhombic natrosilite. In series of 25 mass% Na$_2$O when PbO content decreases in samples, the crystallization of monoclinic natrosilite increases and crystallization of orthorhombic natrosilite decreases. In case of samples with 25 mass% Na$_2$O and high SiO$_2$, the peak intensities are of three or four times higher showing a better crystallization degree.

In both series with 21 mass% Na$_2$O and 25 mass% Na$_2$O when ratio SiO$_2$/Na$_2$O <1.8 (A3, A2, B2), the composition promotes the crystallization of monoclinic natrosilite, while at a ratio SiO$_2$/Na$_2$O >1.8 (B3, D1, D3) the crystallization of orthorhombic natrosilite was preferential.

In order to get more information about the structural modifications, parent glasses and treated samples were analysed by FT-IR spectroscopy.

Infrared spectroscopy (FT-IR)

In Fig. 4a–c, the infrared spectra of parent glasses, samples treated at 400 °C ($T_g$) and samples treated at 650 °C ($T_c$) are shown. All spectra have the characteristic shapes of

**Table 3** Main characteristic bands in FT-IR spectra of heat-treated samples

| Frequencies observed in FT-IR spectra after treatment at 650 °C/cm$^{-1}$ | | | | | | Assignment |
|---|---|---|---|---|---|---|
| A3 | B3 | A2 | B2 | D1 | D3 | |
| 1,146 | 1,141 | 1,151 | 1,146 | 1,146 | 1,146 | SiO$_2$ network in alkali silicate glass [18] |
| | | | | 1,120 | | SiO$_2$ network [18] |
| 1,072 | | 1,072 | 1,072 | 1,072 | 1,060 | SiO$_2$ network [18] |
| 1,053 | 1,053 | 1,053 | 1,053 | 1,053 | | SiO$_2$ network [18] |
| 1,024 | 1,027 | 1,022 | 1,024 | 1,024 | 1,024 | Si–O– bond |
| | 1,012 | | | | 1,012 | Si–O– bond |
| 982 | | 986 | 984 | 984 | 986 | Si–O– bond |
| 967 | 970 | 965 | 967 | 970 | 970 | Si$_2$O$_7^{-6}$ in barysilite [17] |
| | | 898 | | | | Si$_2$O$_7^{-6}$ in barysilite [17] |
| 872 | | 874 | | | | Si$_2$O$_7^{-6}$ in barysilite [17] |
| 767 | 770 | 770 | 770 | 770 | 770 | Si$_2$O$_7^{-6}$ in barysilite [17] |
| 758 | | 753 | 753 | 756 | | SiO$_4$ in chains [6] |
| | 743 | | | 741 | 741 | SiO$_4$ in chains [6] |
| 710 | 710 | 710 | 710 | 710 | 710 | SiO$_4$ in chains [6] |
| 608 | 608 | 605 | 608 | 605 | 605 | SiO$_4$ in chains [6] |
| 584 | | 586 | | | | SiO$_4$ in chains [6] |
| 543 | | 546 | 543 | 543 | | Si–O– bond |
| 512 | 512 | 510 | 510 | 512 | 512 | SiO$_4$ in silicates [9] |
| 489 | 489 | 489 | 489 | 489 | 489 | SiO$_4$ in silicates [9] |
| 463 | 465 | 463 | 463 | 463 | 479 | Si–O-Pb in barysilite [17] |
| 412 | 408 | 415 | | | 408 | Pb–O in barysilite [17] |

glasses containing the main broad bands in the range 800–1,300 cm$^{-1}$, bands in the range 600–750 cm$^{-1}$, and bands below 500 cm$^{-1}$. The presence of the band near 1,640 cm$^{-1}$ is assigned to the vibration of adsorbed water from air during the preparation of the transparent pellet during mixing and vacuum pressing. The characteristic bands for samples treated at 650 °C are presented in Table 3.

The broad bands in the range 800–1,300 cm$^{-1}$ indicate different structural orderings of the glass network due to overlapping of stretching vibrations of various silicate units. This behavior can be influenced by quantities of PbO and Na$_2$O in the glass composition. The spectra for parent glasses (Fig. 4a) and spectra of samples treated at 400 °C for 12 h (Fig. 4b) are similar. In case of spectra of samples treated at 650 °C for 12 h (Fig. 4c), the broad band was divided into 7–8 bands. The same behaviour can be seen in case of bands in the ranges 600–750 cm$^{-1}$ and 400–500 cm$^{-1}$. Increasing of ordering in glass network can be observed in FT-IR spectra of samples treated at 650 °C for 12 h when the bands between 600 and 750 cm$^{-1}$ have higher intensities than the same bands in spectra of parent glasses, and the number of bands increased. The number of bands in this range was correlated with crystallization in glasses as other researchers reported [6, 31]. The bands noticed in the range 400–500 cm$^{-1}$ were attributed to Pb–O–Pb and Pb–O–Si bonds according to previous observations [32].

The results of FT-IR spectroscopy are in agreement with XRD and DTA data and all results show that samples after treatment at 400 °C for 12 h have maintained the glassy state, without nucleation, and that crystallization of silicates occurs at temperatures higher than $T_g$. All FT-IR spectra of samples treated at 650 °C for 12 h presented the order of structural elements in good correlation with crystallization effect from DTA curves and with identification of crystalline phases in the XRD patterns.

Morphological observation and EDAX analysis

From the viewpoint of morphology, the parent glasses and samples treated at 400 °C for 12 h have shown the aspect of glassy state (they are not here). All samples treated at 650 °C for 12 h crystallize and their morphology is presented in Fig. 5a–f. Micrometer crystallites dispersed in the glass matrices have affected the transparencies and made the glasses opaque after treatment at 650 °C. SEM micrographs of the A2 and A3 samples treated at 650 °C for 12 h show the glassy state morphology and few crystallites of 1–8 μm. Their shapes and dimensions are different. Figure 6 shows EDAX results recorded on a crystallite in the A2 sample and the composition of natrosilite was evidenced. A similar
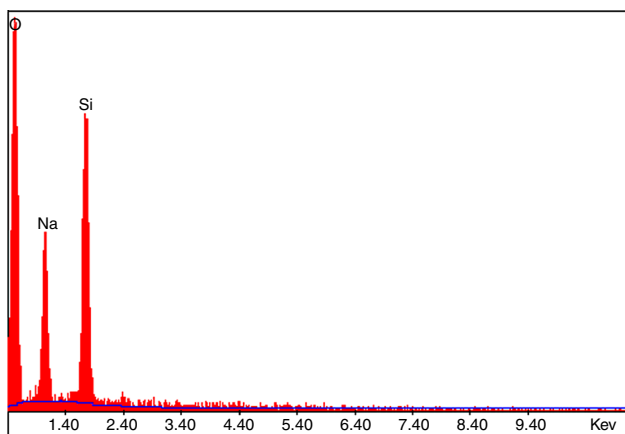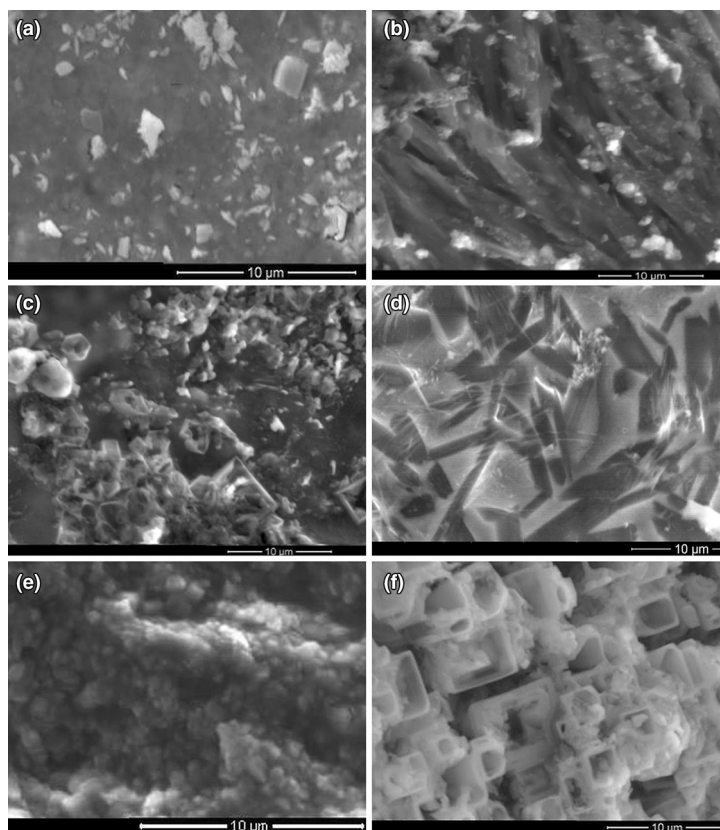
Fig. 6 EDAX image of natrosilite in sample A2 treated at 650 °C for
12 h

morphology can be observed in B3 sample treated at 650 °C
for 12 h and the order of network can be seen in second plan
of image. In D1 sample treated at 650 °C for 12 h, the
number of crystallites increases and the glassy morphology
can be observed just in space between the grains. In case of
D3 sample treated at 650 °C for 12 h, the number of crys-
tallites and their size increases. In D3 sample, the crystallites
are growing on a direction; they are well defined and they
seem to be colourless. The dark colour between the crystal-
lites is glass.

All results from characterization methods were in
agreement and concluded that the crystallization of sodium
disilicate ($Na_2Si_2O_5$) and lead silicate ($Pb_3Si_2O_7$) after
treatment at 650 °C for 12 h occurs. The polymorph phase
of disilicate was orthorhombic when the silica content was
with 9 mass% more than lead oxide content in composition
and monoclinic in other samples where the gap was less
than 5 mass%.

## Conclusions

The crystallization of samples in ternary $Na_2O$–$SiO_2$–PbO
glass system was studied. DTA, XRD and FT-IR mea-
surements confirmed the amorphous state of parent glasses
and of glasses treated at 400 °C for 12 h and the formation
of silicates in samples treated at 650 °C for 12 h.

Samples with content of PbO higher than the content of
$SiO_2$ (A3 and A2) have presented low crystallization ten-
dency. When ratio between them is changed, the lead
becomes modifier and the crystallization tendency increa-
ses. Samples with 21 % $Na_2O$ have shown a crystallization
tendency lesser than samples with content of 25 % $Na_2O$.

A high content of lead oxide in composition can involve
in obtaining monoclinic natrosilite in crystallized samples
as it was discovered in A2 and A3 glasses.

## References

1. Fernandes HR, Tulyaganov DU, Ferreira JMF. $Al_2O_3/K_2O$-containing non-stoichiometric lithium disilicate-based glasses. A study of crystallisation kinetics. J Therm Anal Calorim. 2013;112: 1359–68.

2. Lendvayova S, Moricova K, Jona E, Uherkova S, Kraxner J, Pavlík V, Durny R, Mojumdar SC. Thermal properties of oxide glasses. Part V. Effect of added CoO and NiO oxides on the thermal stability of $Li_2O$–$2SiO_2$ glass system. J Therm Anal Calorim. 2013;112:1133–6.

3. Mastelaro VR, Zanotto ED, Lequeux N, Cortes R. Relationship between short-range order and ease of nucleation in $Na_2Ca_2Si_3O_9$, $CaSiO_3$ and $PbSiO_3$ glasses. J Non-Cryst Solids. 2000;262: 191–9.

4. Fokin VM, Potapov OV, Zanotto ED, Spiandorello FM, Ugolkov VL, Pevzner BZ. Mutant crystals in $Na_2O·2CaO·3SiO_2$ glasses. J Non-Cryst Solids. 2003;331:240–53.

5. Zahra AM, Zahra CY, Piriou B. DSC and Raman studies of lead borate and lead silicate glasses. J Non-Cryst Solids. 1993;155:45–55.

6. Furukawa T, Brawer SA, White WB. Raman and Infrared spectroscopic studies of the crystalline phases in the system $Pb_2SiO_4$–$PbSiO_3$. J Am Ceram Soc. 1979;62:351–6.

7. Sitarz M, Bulat K, Szumera M. Influence of modifiers and glass-forming ions on the crystallization of glasses of the $NaCaPO_4$–$SiO_2$ system. J Therm Anal Calorim. 2012;109:577–84.

8. Ryall WR, Threadgold IM. Evidence for $[(SiO_3)_5]$ infinity type chains in inesite as shown by x-ray and infrared absorption studies. Am Mineral. 1966;51:754–60.

9. Păcurariu C, Lazău RI, Lazău I, Ianos R, Tita B. Non-isothermal crystallization kinetics of some basaltic glass–ceramics containing $CaF_2$ as nucleation agent. J Therm Anal Calorim. 2009;97:507–13.

10. Atkinson I, Teoreanu I, Mocioiu OC, Smith ME, Zaharescu M. Structure property relations in multicomponent oxide systems with additions of $TiO_2$ and $ZrO_2$ for glaze applications. J Non-Cryst Solids. 2010;356:2437–43.

11. Sitarz M, Bulat K, Wajda A, Szumera M. Direct crystallization of silicate–phosphate glasses of $NaCaPO_4$–$SiO_2$ system. J Therm Anal Calorim. 2013;. doi:10.1007/s10973-013-3240-y.

12. Păcurariu C, Lazău RI, Lazău I, Stoleriu S. Kinetic study of the crystallization processes of some decorative ceramic glazes. J Therm Anal Calorim. 2007;88:641–5.

13. Atkinson I, Smith ME, Zaharescu M. Examining correlations between composition, structure and properties in zircon-containing raw glasses. Ceram Int. 2012;38:1827–33.

14. Salagram M, Prasad VK, Subrahmanyam K. IR and optical study of PbO (2PbO·PbO) glass containing a small amount of silica. J Alloys Compd. 2002;335:228–32.

15. Lyon RJP. Infra-Red confirmation of 6-fold co-ordination of silicon in stishovite. Nature. 1962;196:266–7.

16. Craievich AF, Zanotto ED, James PF. Kinetics of sub-liquidus phase separation in silicate and borate glasses. A review. Bull Mineral. 1983;106:169–84.

17. Muller E, Heide K, Zanotto DE. Influence of cation coordination on nucleation in silicate glasses. Zeitschrift fur Kristallographie. 1992;200:287–94.

18. Fokin VM, Potapov OV, Chinaglia CR, Zanotto ED. The effect of pre-existing crystals on the crystallization kinetics of a soda–lime–silica glass The courtyard phenomenon. J Non-Cryst Solids. 1999;258:180–6.

19. Wittman E, Zanotto ED. Surface nucleation and growth in Anorthite glass. J Non-Cryst Solids. 2000;271:94–9.

20. Zanotto ED. Isothermal and adiabatic nucleation in glass. J Non-Cryst Solids. 1981;89:361–70.

21. Mocioiu OC, Zaharescu M, Jitianu G, Budrugeac P. Kinetic parameters determination in non-isothermal conditions for the crystallizations of a silica–soda–lead glass. J Therm Anal Calorim. 2006;86:429–36.

22. Constantinescu M, Olteanu M, Nuta I, Mocioiu OC, Britchi M, Zaharescu M. Inertization of some industrial wastes with high PbO content by vitrification. Proceedings of the 8th Conference of oxide materials science and engineering. 2000; II:214-9.

23. AcerS-NIST, Phase Equilibria Diagrams, Fig. 00494.

24. Kruger H, Kahlenberg V, Kaindl R. Structural studies on $Na_6Si_8O_{19}$ a monophyllosilicate with a new type of layered silicate anion. Solid State Sci. 2005;7:1390–6.

25. Williamson J, Glasser FP. Phys Chem Glasses. 1966;7:127–38.

26. Kahlenberg V, Dorsam G, Wendschuh-Josties M, Fischer RX. The crystal structure of δ-$Na_2Si_2O_5$. J Solid State Chem. 1999; 146:380–4.

27. Rakic S, Kahlenberg V, Weidenthaler C, Zibrowius B. Structural characterization of high-pressure C-$Na_2Si_2O_5$ by single-crystal diffraction and 29Si MAS NMR. Phys Chem Minerals. 2002;29: 477–84.

28. Shahid KA, Glasser FP. Phase equilibriums in the glass-forming region of the system sodium oxide–calcium oxide–silicon dioxide. Phys Chem Glasses. 1971;12:50–7.

29. Dolejs D, Baker DR. Thermodynamic analysis of the system $Na_2O$–$K_2O$–CaO–$Al_2O_3$–$SiO_2$–$H_2O$–$F_2O_{-1}$: Stability of fluorine-bearing minerals in felsic igneous suites. Ed. e-Print Network 2003. pp. 1-12.

30. Bjorkman B, Eriksson G, Rosen E. Generalized approach to the flood-Knapp structure based model for binary liquid silicates: application and update for the PbO–$SiO_2$ system. Metall Trans B. 1984;15B:511–6.

31. Suzuki T, Arai Y, Ohishi Y. Crystallization processes of $Li_2O$–$Ga_2O_3$–$SiO_2$–NiO system glasses. J Non-Cryst Solids. 2007;353: 36–43.

32. Mocioiu OC, Popa M, Neacsu EI, Zaharescu M. Correlation of structural units and chemical stability in $SiO_2$–PbO–$Na_2O$ ternary glasses: spectroscopic methods. J Non-Cryst Solids. 2013;361: 130–41.